COMPUTER ANALYSIS OF MULTICIRCUIT SHELLS OF REVOLUTION BY THE FIELD METHOD

G.A. COHEN

Structures Research Associates, Laguna Beach, California 92651, U.S.A.

SUMMARY

Conventional methods of numerical analysis of the response of axisymmetric shell structures suffer from several practical difficulties. In the finite-difference methods one must choose in advance the finite-difference mesh points. It need only be noted here that too few mesh points result in excessive truncation error, whereas too many mesh points result in excessive round-off error. In the superposition methods, which employ forward integration techniques, the meridian of the shell must be artificially subdivided into a number of "suitably small" subintervals in order to circumvent the inherent instability of these methods. A shell subdivision set up for one mode of response may fail for a different mode of response simply because what is "suitably small" for one problem may be "too long" for another.

The method of analysis developed in this paper is designed to overcome these difficulties. This method, which has been termed the "field method", converts the boundary-value problem into two successive initial-value problems. In the first initial-value problem, a forward integration over the shell meridian is made for the "field functions", which may be interpreted physically as influence functions (plus additional functions to account for external loading) of the structure. The second initial-value problem consists of a backward integration (i.e., in the reverse direction) for the physical force and displacement functions, the differential equations for which are dependent on the already calculated field functions. In this method, no artificial subdivision of the meridian is necessary since both initial-value problems are numerically stable. Also, because the physical response functions are obtained directly from the backward integration, their storage points may be chosen automatically during execution to obtain a uniformly "dense" description of these functions.

Studies comparing the efficiency (i.e., execution time) of the field method with that of a conventional superposition (Zarghamee) method have been made. For the simple case of the linear static response of a clamped cylindrical shell with $l/r=1$, $r/t=10^3$ subjected to uniform pressure loading, the field method is as much as 2.7 times faster than the superposition method when the circumferential wave number is increased to 500, at which point the superposition method broke down due to insufficiently short subintervals. For $l/r=10$ and axisymmetric uniform pressure loading, the field method is as much as 6 times faster when r/t is increased to 10^4, at which point the superposition method had broke down.

The field method has been presented previously for shells of revolution with open branched meridians. The main purpose of the present paper is to extend this work to the case of meridians which contain circuits. Also, a new method for the treatment of arbitrary kinematic constraints is presented.

1. Introduction

This paper is a sequel to an earlier paper [1] in which it is shown how even-order linear boundary-value problems defined on trees (see [1] for definition of terms borrowed from graph theory) may be formulated as two successive initial-value problems. In contrast to conventional superposition methods of numerical integration of such problems, the resulting initial-value problems are numerically stable, thereby eliminating the need for artificial subdivision of the tree into a number of sufficiently small segments. This method of solution has been termed the field method; however, it is known in disciplines other than structural mechanics as one form of the technique of invariant imbedding [2]. Although there are alternate forms of invariant imbedding which eliminate the backward integration of the field method [3], they suffer from the need of having to choose in advance the set of response storage points. In the field method, since the response functions are obtained directly from the backward integration, their storage points may be chosen automatically so as to obtain a uniform description of these functions. Furthermore, in many cases, the extra work done in the forward integration of the alternate methods more than compensates for the elimination of the backward integration.

Whereas the analysis of [1] is limited to boundary-value problems defined on trees, the present analysis treats a much broader class of connected graphs which may contain multiple circuits. (In this paper, the term "circuit" will mean a *simple*, i. e., non-self-intersecting, closed chain.) For each arc of the graph, the arc distance s will be used as the independent variable. Let us assume that the arcs have been ordered and oriented with respect to the direction of increasing s, but defer for the time being the manner in which this is done.

2. Definition of Boundary-Value Problem

A system of ordinary differential equations of order $2p$ may always be written as a system of $2p$ first-order equations. If we group one-half of the dependent variables in the $p \times 1$ matrix y and the other half in the $p \times 1$ matrix z, the system of first-order equations may be written, for linear systems, as two matrix differential equations, viz.

$$y' + ay + bz = f \tag{1a}$$

$$z' + cy + dz = g \tag{1b}$$

where prime denotes differentiation with respect to s; a, b, c, d are $p \times p$ matrix functions of s; and f, g are $p \times 1$ matrix functions of s.

Equations (1) are defined at every interior point of each arc of the graph. They are supplemented by linear boundary conditions, defined at the vertices of the graph, of the form

$$B\Delta y + Dz = L \tag{2}$$

where B and D are $p \times p$ matrices, L is a $p \times 1$ matrix, and

$$\Delta y = \sum y^{+} - \sum y^{-} \tag{3}$$

Here, y^{+} and y^{-} represent the values of y at the vertex on exiting and entering arcs, respectively. As implied by the form of eq. (2), it is assumed that z is continuous at vertices. A vertex and its boundary condition are said to be singular if the matrix B is singular; otherwise they are called regular. (In structural mechanics problems, y is a

force vector, z is a displacement vector, and a singular boundary condition corresponds to kinematic constraint.)

The majority of boundary-value problems in mechanics are self-adjoint. This property is synonymous with being derivable from a variational principle. Physically, this corresponds to systems which do not involve energy losses. For the system defined by eqs. (1) and (2), the conditions of self-adjointness are known to be

$$b = b^T, \qquad c = c^T, \qquad d = -a^T \tag{4a}$$

$$\kappa = \kappa^T \tag{4b}$$

where

$$\kappa = B^{-1}D \tag{5}$$

and the superscript T denotes matrix transpose. Although condition (4b) strictly applies only to regular vertices, it may be used also for singular vertices if a singular vertex is viewed as a limiting case of a sequence of regular vertices. Thus, for self-adjoint problems a singular vertex is the limit of a sequence of regular vertices, for each of which eq. (4b) holds true.

3. Field Relations

An *open branch arc* is characterized by the fact that a cut at any of its points disconnects the graph into two separate parts. Conversely, a (single) cut of a *closed branch arc*, which, by definition, lies in a circuit, does not disconnect the graph. However, in order to develop *field relations*, it is necessary to visualize disconnecting the graph by a cut at a generic point. For this purpose, the concept of an *initial point*, denoted henceforth by *I.P.*, of a closed branch arc is introduced. For each closed branch arc, the *I.P.* is chosen so that cuts at the *I.P.* and a generic point, denoted by *G.P.*, of the arc disconnect the graph into two separate parts. Note that the *I.P.* of a given closed branch arc is located in a circuit containing the given arc but not necessarily in that arc itself, and in fact several closed branch arcs lying in the same circuit may have the same *I.P.* (Fig. 1).

Since cuts at the *I.P.* and *G.P.* of a closed branch arc disconnect the graph into two separate parts, it is clear that the values $z = z_0$ at the *I.P.* and $z = z$ at the *G.P.* can serve as boundary conditions which, together with the differential equations (1) and given boundary conditions (2) over one of the parts, determine y and z over that part independently of the corresponding data over the remaining part. In particular, the values z_0 and z determine the values of y at the cuts, which for linear problems is expressed by the matrix relations

$$y = uz + vz_0 + w \tag{6a}$$

$$-y_0^+ = \delta z + \gamma z_0 + \lambda \tag{6b}$$

where u, v, δ, γ are $p \times p$ matrices and w, λ are $p \times 1$ matrices. Equations (6) are the field relations for closed branch arcs, which generalize eq. (6) of [1] for open branch arcs, viz.

$$y = uz + w \tag{7}$$

In eq. (6b), y_0^+ represents the value of y at the *I.P.* on an exiting closed branch arc, which shall be called an *initial closed branch arc*. [All nonsubscripted variables in eqs.

(6) are understood to be evaluated at the *G.P.*] Thus, by definition, the *I.P.* of an initial closed branch arc coincides with its initial vertex. In order to obtain an initial-value problem for the field functions u, v, w, δ, γ, λ, closed branch arcs are ordered and oriented so that for every cut pair all of one part of the disconnected graph is completely described by s-values smaller than that at the *G.P.* (Fig. 1).

For self-adjoint problems, to which our attention is henceforth confined, the matrix K defined by

$$K = \begin{bmatrix} u & v \\ \delta & \gamma \end{bmatrix} \tag{8}$$

represents a stiffness matrix for the part of the disconnected graph which is fully described by s-values smaller than s at the *G.P.* Since such a stiffness matrix is known to be symmetric, its submatrices satisfy the following reciprocal relations

$$u = u^T, \qquad \gamma = \gamma^T, \qquad \delta = v^T \tag{9}$$

Thus, for example, for eighth-order boundary-value problems, there are 44 independent scalar field functions contained in eqs. (6). However, as shown below, only 30 of them (u, v, w) need be stored.

4. Plan of Field Method

Before describing the differential equations and initial values for the field functions, in order to put the discussion in context, a preview of the field method for a graph with circuits is presented. The calculation procedure consists of the following three basic steps (Fig. 2).

I A forward integration is performed over the graph for u, w on open branch arcs and u, w, v, γ, λ on closed branch arcs. On open branch arcs u, w are stored, and on closed branch arcs u, w, v are stored.

II Upon reaching the final vertex, in principle, two cases must be distinguished. If the final arc is an open branch arc or a closed branch arc whose *I.P.* coincides with its terminal vertex, the field relations and boundary conditions at the final vertex are solved simultaneously to give the value of z, say z_1, at the final vertex. If, on the other hand, the final arc is a closed branch arc whose *I.P.* is distinct from its terminal vertex, then the field relations and boundary conditions at the *I.P.* and the final vertex are solved simultaneously to give z_1 and the value of z at the *I.P.*

III Using z_1 as a final value, and z-continuity at interior vertices, a backward integration of the equation [cf. eqs. (1b) and (7)]

$$z' + (cu + d)z = g - cw \tag{10}$$

is performed over the graph. Before integrating eq. (10) on a closed branch arc, w on that arc is replaced by $w + vz_0$ where z_0 is the value of z at its *I.P.* [cf. eqs. (6a) and (7)]. As shown in [4], z_0 for each closed branch arc can be calculated prior to the backward integration on that arc. When a response storage point is reached, y is calculated from the field relation (7).

5. Differential Equations for Field Functions

The differential equations for u, v, w are obtained by the same procedure used in [1] for u, w on open branch arcs. That is, eq. (6a) is differentiated with respect to s, the

differential equations (1) are used to eliminate y' and z', and eq. (6a) is used again to eliminate y. This gives

$$(u' - ucu + au - ud + b)z + (v' - ucv + av)z_0 + w' - ucw + aw + ug - f = 0 \qquad (11)$$

Since eq. (11) must be satisfied identically with respect to z and z_0 (which depend on data at points of greater s, whereas u, v, w do not), it follows that

$$u' - ucu + au - ud + b = 0 \qquad (12a)$$

$$w' - ucw + aw + ug - f = 0 \qquad (12b)$$

$$v' - ucv + av = 0 \qquad (12c)$$

Note that eqs. (12a, b) apply to both open and closed branch arcs, and that eq. (12c) is simply the homogeneous form of eq. (12b).

In a similar manner, to obtain the differential equations for γ, λ, differentiate eq. (6b) with respect to s, and use eq. (1b) to eliminate z' and eq. (6a) to eliminate y. This gives

$$[\delta' - \delta(cu + d)]z + (\gamma' - \delta cv)z_0 + \lambda' + \delta(g - cw) = 0 \qquad (13)$$

Since eq. (13) is also an identity in z and z_0, it yields, in view of eqs. (4a) and (9),

$$\gamma' - v^T cv = 0 \qquad (14a)$$

$$\lambda' + v^T(g - cw) = 0 \qquad (14b)$$

These are remarkably simple differential equations, which may be integrated by quadrature after the integration for v and w is made.

6. Initial Values of Field Functions

The derivation of the initial values of the field functions, required for each arc of the graph, is presented in [4] and is not repeated here. In the derivation, it is necessary to distinguish three different kinds of arcs. These are called: (1) ordinary arcs, (2) initial closed branch arcs, and (3) continuation arcs. It will suffice here to simply present a brief description of each of these arcs. For the associated initial values, see [4].

6.1 Ordinary Arcs

An ordinary arc is either an open branch arc whose initial vertex is incident with no closed branch arcs, or a closed branch arc whose initial vertex is incident with precisely one other closed branch arc which precedes the ordinary arc and enters it initial vertex. For example, in Fig. 1, arc 3 is an ordinary arc. In the case of an ordinary closed branch arc, its *I.P.* is also the *I.P.* of the preceding closed branch arc.

6.2 Initial Closed Branch Arcs

As mentioned earlier, an initial closed branch arc is characterized by the fact that its *I.P.* coincides with its initial vertex. Since the use of a minimum number of initial points leads to the simplest analysis, in general an initial closed branch arc will be any closed branch arc for which no vertex preceding its initial vertex can serve as its *I.P.* A sufficient condition for a closed branch arc to be an initial closed branch arc is that its initial vertex is incident with another closed branch arc which lies in a common circuit and is either an exiting arc or an entering but not preceding arc. For example, in Fig. 1, arcs 1, 2, 4, and 6 are initial closed branch arcs.

6.3 Continuation Arcs

A continuation arc is defined simply as any arc not of the preceding two types. It is therefore either an open branch arc whose initial vertex is incident with a closed branch arc, or a closed branch arc (other than an initial closed branch arc) whose initial vertex is incident with more than one other closed branch arc. For example, in Fig. 1, arcs 5 and 7 are continuation arcs. (The name "continuation arc" was chosen since such an arc can be thought of as an arc which continues a path which has been interrupted by a circuit.)

7. Shells of Revolution

The computer program described in [1] for shells of revolution for which the reference meridian is a tree has been extended to multicircuit meridians. This program calculates the linear elastic response of ring-stiffened shells to mechanical and thermal loads which vary harmonically in the circumferential direction. The differential equations (1) are eighth-order so that the response matrices y and z are 4-element column vectors. The equations are ordered so that y and z are the force and displacement (amplitude) vectors

$$y^T = r(P,\ Q,\ S,\ M_1) \tag{15a}$$

$$z^T = (\xi,\ \eta,\ v,\ \chi) \tag{15b}$$

where P, Q, S are forces per unit of circumferential length referred to fixed axial, radial, and circumferential coordinate directions, respectively; ξ, η, v are the corresponding displacement components; M_1 is the meridional bending moment per unit of circumferential length; χ is the corresponding rotation; and r is the local small circle radius. The matrices a, b, c, f, g of the differential equations, as well as $\kappa = B^{-1}D$ and $B^{-1}L$ for ring boundaries, are given in [4].

7.1 Example

A solution of the shell equations by the field method for a multicircuit meridian (Fig. 3) is presented in this section. In order to have a quantitative check on the accuracy of the numerical solution, the structure was devised to have a plane of symmetry normal to the axis of revolution. (In practice, only one-half of a symmetrical structure would be modeled.) Thus, the accuracy of the solution can be checked simply by comparing the calculated response at symmetry points. Shown in Fig. 3 are harmonic pressure load amplitudes (underlined) and entry, i. e., output station, numbers. Equally spaced output stations corresponding to intervening integral entry numbers are not shown. As is shown, the meridian consists of six arcs, the orientation and order of which are indicated by the arrow on each arc and the adjacent number. In the calculation the circumferential harmonic number of the pressure loading and response was $n = 1000$, and the following homogeneous, isotropic wall properties were assumed: $E = 10^7$, $\nu = 0.25$, $t = 0.1$. These properties and the dimensions and pressure amplitudes shown in Fig. 3 may be taken to be in any consistent set of units.

This problem has been run in single precision on the UNIVAC 1108 computer (a 36-bit word machine) with no degradation of accuracy relative to the CDC 6600 computer (a 60-bit word machine). Therefore, it follows that the small numerical discrepancies which occur at symmetry points (see Table I, reproduced from a computer print-out with an added column labeled "SYM. POINT" giving the entry number of the symmetry point for each output station)

are due essentially to truncation error, which is controlled by an input truncation error tolerance, and that round-off errors are negligible. In the calculation the truncation error tolerance was set to 10^{-3}, which means that the size of each numerical integration step was adjusted so that an estimate of the error introduced into each dependent variable by that integration step was less than 0.001 of the value of the variable. Inspection of the calculated response functions in Table I shows that, except in the immediate vicinity of their zeroes, they retain this degree of accuracy, viz. three significant digits. The UNIVAC 1108 central processor time expended in obtaining these results was 14.8 seconds.

7.2 Comparison with a Superposition Method

In superposition methods, which employ forward integration techniques, the truncation error is controlled automatically by the use of self-checking variable step-size integration routines. However, since the auxiliary solutions exhibit exponential growth characteristics, their superposition involves large round-off errors at points remote from the initial point of integration. To circumvent this problem, the meridian of the shell is artificially subdivided into a number of "suitably small" segments. Nevertheless, a shell subdivision set up for one mode of response may fail for a different mode of response simply because what is "suitably small" for one problem may be "too long" for another.

The field method not only retains the feature of automatic control of truncation error, but also produces stable initial-value problems whose solutions are not sensitive to small numerical errors introduced at each integration step. Consequently, no artificial subdivision of the shell meridian is required, leaving the user free from concerns of numerical convergence or ill-conditioning. This is illustrated in Fig. 4, showing computation times for the calculation of the linear elastic response of a pressurized clamped cylinder by the field method and also by an efficient superposition method, known as the Zarghamee-Robinson method [5-7]. The bar graph [Fig. 4(a)] compares the computational efficiencies of the two methods in terms of CDC 6600 CPU seconds for the axisymmetric response for several radius-to-thickness ratios. In each case the field method is significantly more efficient. More important is the fact that, even with 33 segments, the superposition method failed to give meaningful results at $r/t = 10^4$, whereas the field method experienced no difficulty with no subdivision. Similar results are obtained when the circumferential wave number is varied, as shown in Fig. 4(b).

ACKNOWLEDGEMENT

This work was supported by the National Aeronautics and Space Administration under Contract NAS1-12764. The author is indebted to Dr. Wendell B. Stephens of the NASA Langley Research Center for providing the results shown in Fig. 4.

REFERENCES

[1] COHEN, G. A., "Numerical Integration of Shell Equations Using the Field Method," *Journal of Applied Mechanics*, Vol. 41, No. 1, Mar 1974, pp. 261-266.

[2] SCOTT, M. R., "A Bibliography on Invariant Imbedding and Related Topics," Rep. SLA-74-0284, Sandia Laboratories, June 1974.

[3] SCOTT, M. R., "On the Conversion of Boundary-Value Problems into Stable Initial-Value Problems via Several Invariant Imbedding Algorithms," Rep. SAND74-0006, Sandia Laboratories, July 1974.

[4] COHEN, G. A., "Computer Analysis of Multicircuit Shells of Revolution by the Field Method, NASA CR-2535, 1975.

[5] GOLDBERG, J. E., SETLUR, A.V., ALSPAUGH, D. W.,"Computer Analysis of Non-Circular Cylindrical Shells," Intl. Symp. on Shell Structures in Engineering Practice, Budapest, Hungary, Aug 31 - Sept 3, 1965.

[6] ZARGHAMEE, M. S., ROBINSON, A. R., "A Numerical Method for Analysis of Free Vibrations of Spherical Shells," *AIAA Journal*, Vol. 5, No. 7, July 1967, pp. 1256-1261.

[7] COHEN, G. A., "Computer Analysis of Ring-Stiffened Shells of Revolution," NASA CR-2085, 1973.

TABLE I CALCULATED FORCE AND DISPLACEMENT AMPLITUDES

SYM. POINT	ENTRY	S	P	Q	CAP S	M1	XI	ETA	V	CHI
21	1	0.0000	9.7331+01	2.8107+01	-4.8403+01	6.6246+00	1.2168-04	-1.0245-03	4.0175-05	3.8308-04
22	2	7.8540-01	4.6748+01	4.7740+01	-5.0872+01	-1.7144+00	-1.6900-04	-1.7249-04	4.3008-05	8.3367-04
23	3	1.5708+00	-2.6878-03	4.2715+01	-1.5167-01	-4.0169-01	-3.4247-04	-3.2087-08	9.6189-05	1.5466-07
24	4	2.3562+00	-4.6705+01	4.7723+01	5.0520+01	-1.7115+00	-1.6911-04	1.7262-04	4.2146-05	-8.3361-04
25	5	3.1416+00	-9.7095+01	2.8024+01	4.8029+01	6.6106+00	1.2193-04	1.0242-03	3.8441-05	-3.8344-04
16	6	3.1416+00	-6.1340+01	5.7636+01	-1.3196+02	-1.3600+01	1.2168-04	-1.0245-03	4.0175-05	3.8308-04
17	7	3.9270+00	1.2578+01	-1.3813+01	-1.0728+02	2.8221+00	5.1931-04	-7.4052-05	8.2680-05	-8.5771-04
18	8	4.7124+00	8.9391-03	-6.7509+01	-1.9449-01	-2.3137-01	6.2274-04	-2.3280-07	1.4440-04	-1.3442-06
19	9	5.4978+00	-1.2639+01	-1.3853+01	1.0699+02	2.8249+00	5.2038-04	7.3204-08	8.2018-05	8.5758-04
20	10	6.2832+00	6.1275+01	5.7645+01	1.3184+02	-1.3807+01	1.2193-04	1.0242-03	3.8441-05	-3.8344-04
15	11	6.2832+00	-3.5979+01	-8.5719+01	1.8037+02	6.9733+00	1.2168-04	-1.0245-03	4.0175-05	3.8308-04
14	12	7.3939+00	-2.3657+02	-9.2519+01	1.0563+02	-2.1964+00	4.5534-04	-1.7267-03	-4.3808-05	-5.2608-04
13	13	8.5046+00	-3.1080+02	3.2243-03	4.9967-03	1.5130+00	1.5605-07	-1.0748-03	-3.4381-05	-1.2270-06
12	14	9.6153+00	-2.3661+02	9.2539+01	-1.0549+02	-2.1949+00	-4.5527-04	-1.7267-03	-4.3587-05	5.2457-04
11	15	1.0726+01	-3.5998+01	8.5739+01	-1.8034+02	6.9781+00	-1.2167-04	-1.0245-03	4.0154-05	-3.8304-04
6	16	1.0726+01	6.1337+01	5.7637+01	-1.3195+02	1.3601+01	-1.2167-04	-1.0245-03	4.0154-05	-3.8304-04
7	17	1.1511+01	-1.2578+01	-1.3812+01	-1.0728+02	-2.8221+00	-5.1938-04	-7.3972-08	8.2671-05	8.5803-04
8	18	1.2297+01	-8.4911-03	-6.7503+01	-1.9489-01	2.3111-01	-6.2279-04	-2.0201-07	1.4440-04	1.2482-06
9	19	1.3082+01	1.2644+01	-1.3858+01	1.0697+02	-2.8244+00	-5.2029-04	7.3288-08	8.1972-05	-8.5764-04
10	20	1.3868+01	-6.1267+01	5.7640+01	1.3183+02	1.3606+01	-1.2188-04	1.0242-03	3.8447-05	3.8336-04
1	21	1.4653+01	-9.7339+01	2.8112+01	-4.8402+01	-6.6254+00	-1.2167-04	-1.0245-03	4.0154-05	-3.8304-04
2	22	1.5438+01	-4.6752+01	4.7742+01	-5.0886+01	1.7145+00	1.6904-04	-1.7250-04	4.2998-05	-8.3377-04
3	23	1.6224+01	3.6420-03	4.2719+01	-1.3743-01	4.0210-01	3.4271-04	3.4663-08	9.8199-05	-3.4857-07
4	24	1.7009+01	4.6705+01	4.7722+01	5.0523+01	1.7116+00	1.6909-04	1.7262-04	4.2161-05	8.3362-04
5	25	1.7009+01	9.7107+01	2.8028+01	4.8045+01	-6.6115+00	-1.2188-04	1.0242-03	3.8447-05	3.8336-04
30	26	1.7009+01	3.5839+01	8.5669+01	1.7988+02	6.9947+00	-1.2188-04	1.0242-03	3.8447-05	3.8336-04
29	27	1.8120+01	2.3684+02	9.2612+01	1.0577+02	-2.2070+00	-4.8714-04	1.7289-03	-4.6899-05	-5.2703-04
28	28	1.9231+01	3.1152+02	2.4131-03	1.9466-02	1.5221+00	4.6501-08	1.0730-03	-5.9293-06	6.8881-08
27	29	2.0341+01	2.3683+02	-9.2606+01	-1.0576+02	-2.2070+00	4.8712-04	1.7288-03	-4.6602-05	5.2763-04
26	30	2.1452+01	3.5820+01	-8.5668+01	-1.7987+02	6.9966+00	1.2193-04	1.0242-03	3.8441-05	-3.8344-04

*FIN

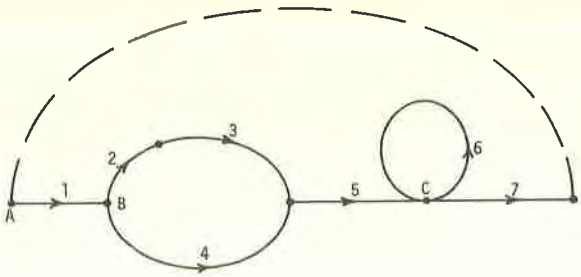

Fig. 1 Illustration of initial points and arc ordering and orientation. Vertex A is the *I.P.* for arcs 1, 5, and 7; vertex B (arc 2) is the *I.P.* for arcs 2 and 3; vertex B (arc 4) is the *I.P.* for arc 4; vertex C is the *I.P.* for arc 6.

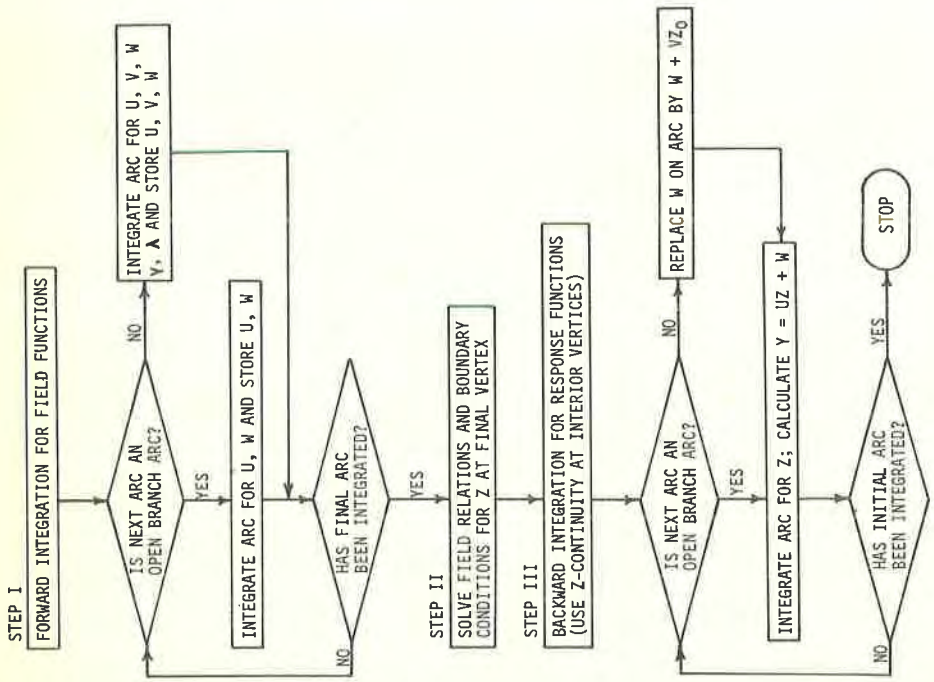

Fig. 2 Flow chart of field method

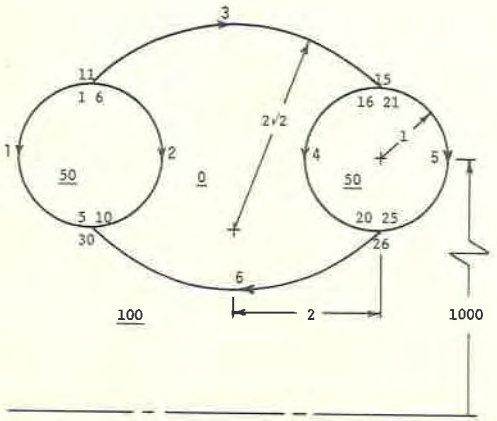

Fig. 3 Example shell configuration

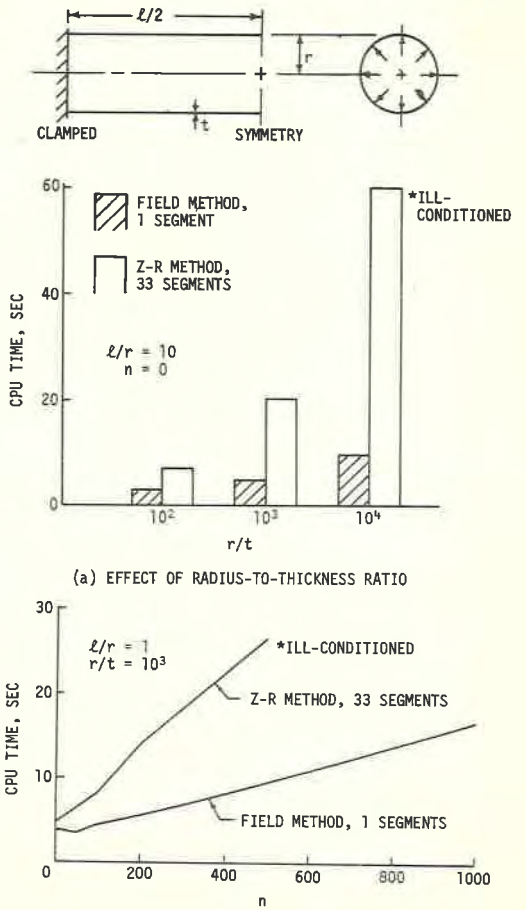

Fig. 4 Computation times of field and Zarghamee-Robinson methods for pressurized cylindrical shells